Image Reconstruction of Shielded Mixed-Oxide Fuel Using a Dual-Particle Imaging System

J. Kyle Polack, *Member, IEEE,* Alexis Poitrasson-Rivière, Michael C. Hamel, Kai Ito, Shaun D. Clarke, Marek Flaska, *Member, IEEE*, Sara A. Pozzi, *Member, IEEE*, Alice Tomanin, and Paolo Peerani

***Abstract*–The dual-particle imaging system being developed at the University of Michigan was used at the Joint Research Centre in Ispra, Italy for measurements on samples of special nuclear material. A 1,150-g mixed-oxide (MOX) fuel sample was measured with various shielding configurations to determine how the presence of lead and/or polyethylene shielding degrades the system's ability to localize a source by simultaneous neutron and photon imaging. Three two-hour measurements were taken with the source shielded by an: a) 8-mm lead sheath and 5.1-cm lead bricks, b) 8-mm lead sheath and 6.5-cm polyethylene bricks, and c) 8-mm lead sheath, 5.1-cm lead bricks, and 6.5-cm polyethylene bricks. The 8-mm lead sheath was used in all cases to reduce the measured photon count rate. A "bare" measurement was also made by using only the 8-mm lead sheath, but the unexpected presence of additional sources has rendered the measurement unsuitable for comparison. The resulting images show that the dual-particle imaging system is able to accurately localize the MOX canister in the presence of intervening material.**

I. Introduction

A dual-particle imaging system is under development at the University of Michigan for the detection, localization, and identification of special nuclear material (SNM) [1-3]. The dual-particle imager (DPI) is capable of imaging both fast neutrons and gamma rays, which increases the probability that the system will detect and localize a neutron/gamma -emitting source when shielding materials are present. Similar systems are being developed at Sandia National Laboratories [4] and the University of New Hampshire [5]. The DPI has been previously tested using the common SNM (^{240}Pu) surrogate, ^{252}Cf. More complex measurements have been simulated using MCNPX-PoliMi [6]. A measurement campaign was recently performed during which the DPI was brought to the Joint Research Centre (JRC) in Ispra, Italy with the goal of measuring various SNM samples. A subset of the measurements focused on the impact that lead and polyethylene shielding have on the ability of the DPI to locate a sample of mixed-oxide (MOX) fuel.

Manuscript received December 20, 2014. This work is supported in-part by the National Nuclear Security Administration through NA-22 funding opportunity DE-FOA-0000568. It is also funded in part by the Consortium for Verification Technology under Department of Energy National Nuclear Security Administration award number DE-NA0002534. The prototype system is funded in part by the Department of Energy, Nuclear Energy University Program, award number DE-NE0000324. J. K. Polack and M. C. Hamel are funded in part by the Sandia National Laboratories Excellence in Engineering Research Fellowship. Sandia National Laboratories is a multi-program laboratory managed and operated by Sandia Corporation, a wholly owned subsidiary of Lockheed Martin Corporation, for the U.S. Department of Energy's National Nuclear Security Administration under contract DE-AC04-94AL85000.

J. K. Polack, A Poitrasson-Rivière, M. C. Hamel, S. D. Clarke, M. Flaska, and S. A. Pozzi are with the University of Michigan Department of Nuclear Engineering and Radiological Sciences, Ann Arbor, MI 48109 USA (e-mail: dnngimaging@umich.edu).

K. Ito is with Nagoya University, Furo-cho, Chikusa-ku, Nagoya, Japan but is currently visiting the University of Michigan Department of Nuclear Engineering and Radiological Sciences, Ann Arbor, MI 48109 USA.

A. Tomanin and P. Peerani are with the Joint Research Center, Ispra, Varese, Italy.

II. Dual-Particle Imaging System

The DPI is a two-plane imaging system that uses Compton- and neutron-scattering physics to detect and locate radioactive sources. The front plane of the system is comprised of a 4×4 array of 5.1-cm-thick by 7.62-cm-diameter EJ-309 liquid organic scintillators. The back plane is comprised of a 4×4 array that includes eight 7.62-cm-thick by 7.62-cm-diameter EJ-309 scintillators and eight 7.62-cm-thick by 7.62-cm-diameter NaI inorganic scintillators arranged in a checkerboard pattern.

The image reconstruction results shown in this paper utilize the simple-backprojection (SBP) method. SBP requires an incident photon or neutron to interact in both the first and second planes to produce an imageable event. When such an event occurs, the energy depositions, detector locations, and time of flight (TOF) between interactions (in the case of neutrons) are used to compute the incoming angle of the detected particle. For photons, the incident angle, θ_γ, is calculated as:

$$\cos\theta_\gamma = 1 - \frac{m_e c^2 \times E_{d1}}{E_{d2}(E_{d1}+E_{d2})} \quad , \tag{1}$$

where E_{d1} and E_{d2} are the energies deposited in the first and the second detector, respectively, m_e is the electron rest mass, and c is the speed of light. For neutrons, the incident angle, θ_n, is calculated as:

$$\cos^2\theta_n = {E_{n1}}/{E_{n0}}, \tag{2}$$

where E_{n1} is the energy of the neutron after interacting in the first detector and E_{n0} is the incident energy of the neutron. E_{n1} can be calculated as:

$$E_{n1} = \frac{m_n}{2} \times \frac{d^2}{TOF^2}, \tag{3}$$

where m_n is the rest mass of a neutron, d is the distance between the detector centers, and TOF is the time of flight between interactions in the first and the second plane. E_{n0} is determined by adding E_{n1} to the energy deposited by the neutron in the first detector.

The incident angle is used to create a cone of possible source locations, which is projected onto a spherical field of view (FOV). After multiple counts are detected, the projected cones overlap and a hotspot forms on the image that signifies the direction of any present source(s).

III. Experimental Methods

A 1,150-g MOX source was measured with the DPI at a distance of 2.5 m. The MOX sample was in a cylindrical canister with a height of 30 cm and a diameter of 13.5 cm. The activity was approximately 28,000 fissions per second and 31,000 (α,n) reactions per second. Material composition and neutron emission fractions of the radioactive isotopes in the MOX sample are shown in Table 1. Oxygen also contributed 16.1 weight % to the mass of the sample. Trace amounts of ^{241}Pu, ^{234}U, and ^{236}U were present in the sample, but did not contribute significantly to either the mass or neutron emission rate.

Table I. MOX Composition and Neutron Emission Fractions

Isotope	Weight %	Neutron %	Neutron Emission Process
^{240}Pu	4.6	58.0	fission
		8.0	(α,n)
^{241}Am	0.5	17.0	(α,n)
^{242}Pu	0.3	7.0	fission
^{238}Pu	0.02	1.0	fission
		4.0	(α,n)
^{239}Pu	10.9	5.0	(α,n)
^{238}U	66.8	~0.0	fission/(α,n)
^{235}U	0.5	~0.0	fission/(α,n)

Three two-hour measurements were performed, each with a different shielding configuration. In one configuration the MOX canister was shielded by 5.1-cm-thick lead bricks. In the second configuration the MOX was shielded by 6.5-cm-thick polyethylene bricks. Finally, the MOX was shielded with both 5.1-cm-thick lead and 6.5-cm-thick polyethylene bricks. In all three cases, the source was contained within an 8-mm-thick lead sheath, which was used to reduce the incident photon count rate to a manageable level. A "bare" (sheath-only) case was also measured for reference. Unfortunately, several strong neutron sources were unknowingly present in the next room during this measurement; the presence of these sources makes the bare case unsuitable for comparison with the shielded cases.

All waveforms were collected using 12-bit, 250-MHz, CAEN V1720 digitizers. During post-processing, 40-keVee thresholds were applied to the pulses collected by the EJ-309s, which provided a good balance between pulse-shape-discrimination capabilities and efficiency. A threshold of 20 keVee was applied to pulses collected by the NaIs.

IV. Results

The neutron SBP images for each of the three measurement configurations are shown in Fig. 1. In all three shielding scenarios, the source is located at an azimuth of 90° and an inclination of 90°. At a distance of 2.5 m, the canister is expected to span approximately 3° in azimuth and 7° in inclination.

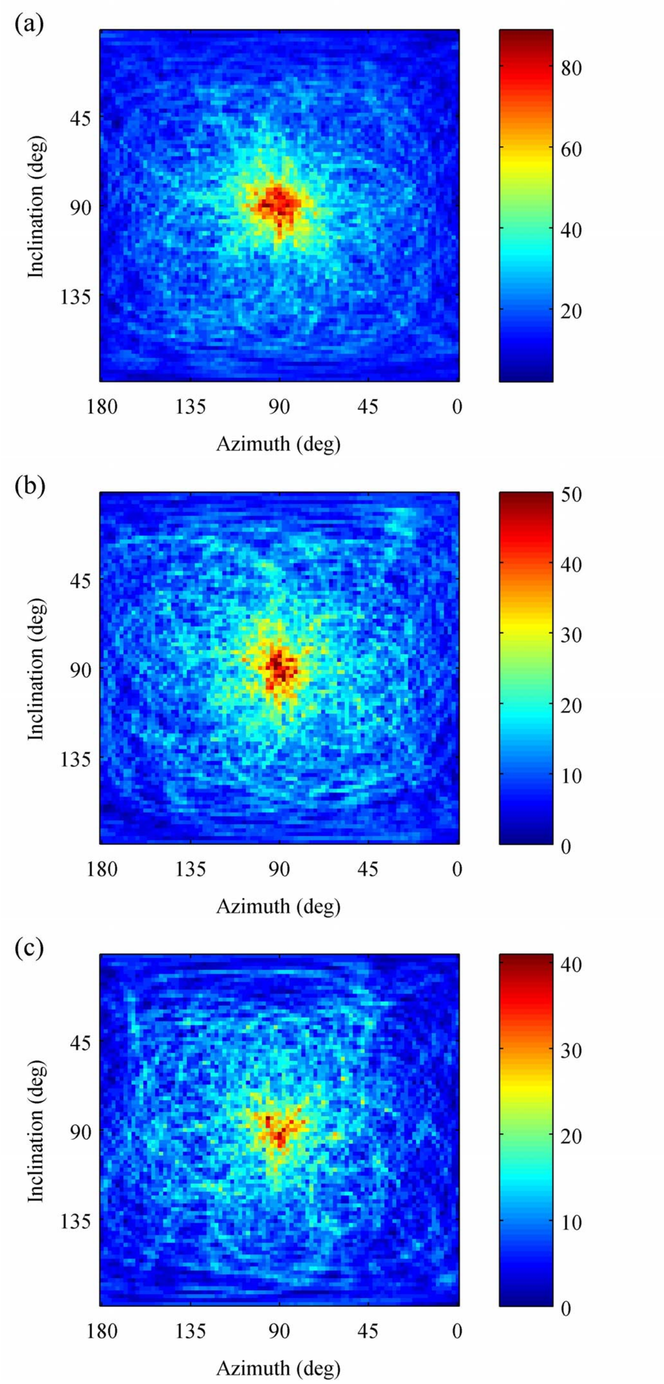

Fig. 1. Neutron SBP images for the (a) lead-shielded, (b) polyethylene-shielded, and (c) combined lead-and-polyethylene-shielded MOX sample. The source is located properly around (90°, 90°) in all three cases.

The neutron images show that the DPI is capable of locating the MOX canister in the presence of lead and/or polyethylene shielding. The image is most converged in the lead-shielded case, while the presence of polyethylene reduced the number of counts in the highest-intensity pixel by approximately a factor of 2. While the canister is only expected to span a 3°×7° portion of the image, the hotspot is blurred by the intrinsic resolution of the DPI, which is approximately 20° for SBP imaging and is due to the combined effects of energy, timing, and spatial (interaction position within a detector) resolution.

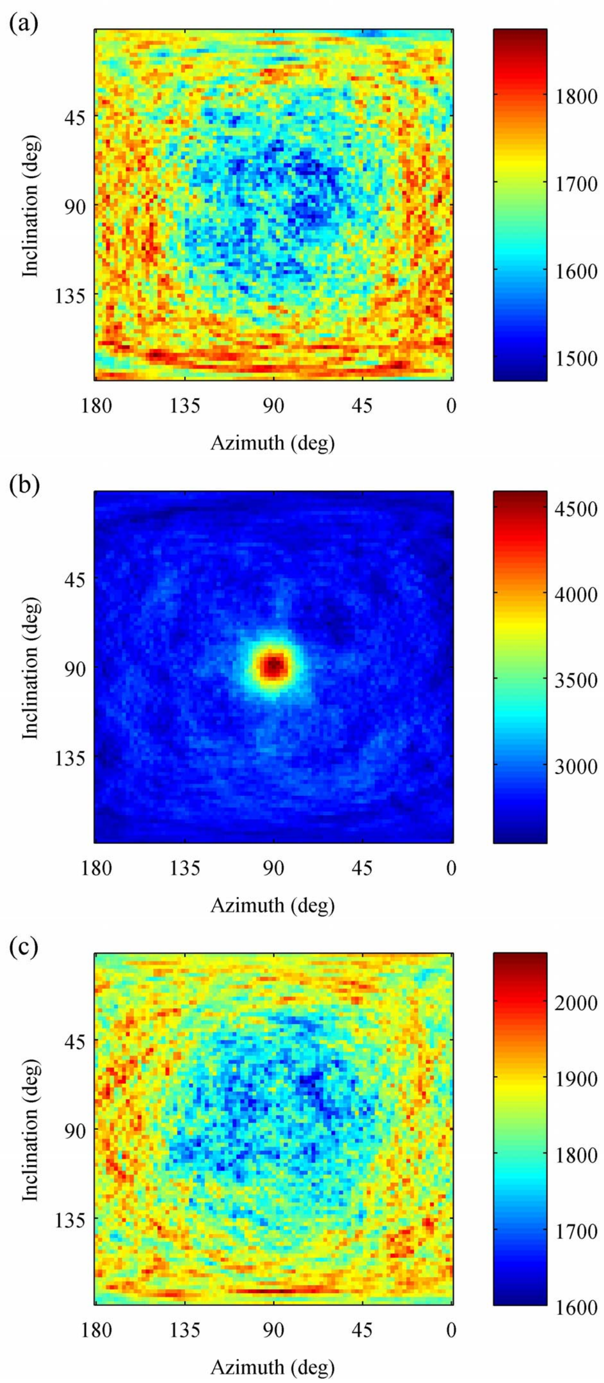

Fig. 2. Photon SBP images for the (a) lead-shielded, (b) polyethylene-shielded, and (c) combined lead-and-polyethylene-shielded MOX sample. The source is only located in (b), while the images shown in (a) and (c) are dominated by background counts.

The photon SBP images for each of the three measurements are shown in Fig. 2. These images clearly show that the source is not detected above background levels when the lead bricks are shielding the source; however, when only the polyethylene bricks are present, a well-converged hotspot appears at the correct source location. Similarly to the neutron SBP images, the intrinsic resolution of the DPI causes the hotspot to span a larger area than the expected 3°×7°.

As expected, the photon SBP images have a much higher contribution from background radiation than the neutron SBP images. The "bowl" shape displayed in Figs. 2(a) and 2(c) is in part due to the photomultiplier tubes facing outward from the front plane. This PMT orientation was chosen to reduce the likelihood of an incident particle scattering in between interactions in the front and back plane; however it reduces the efficiency of the DPI in the forward direction. The larger intensity at the bottom of the "bowl" is due to background radiation emitted from the floor as well as photons that have scattered off the floor prior to being detected.

TABLE 2. MEASURED NEUTRON AND PHOTON COUNT RATES

	Lead Shielded	Polyethylene Shielded	Lead and Poly. Shielded
Neutrons/second	0.161±0.005	0.083±0.003	0.061±0.003
Photons/second	69.642±0.103	97.001±0.116	69.763±0.098

The observed neutron and photon count rates and their associated errors are shown in Table 2. The neutron count rate is highest in the lead-shielded case, and is significantly reduced in the presence of polyethylene. This reduction in count rate is expected due to the high cross section for neutron elastic scattering in hydrogenous material, such as polyethylene. The neutron count rate in the combined-shielding scenario is slightly lower than in the polyethylene-only case because scattering in the lead bricks reduces the number of neutrons that reach the system above threshold. The photon count rate is highest when only the polyethylene shielding is present, which is expected due to the high Compton scatter and photoelectric absorption cross sections of lead. The photon count rates for the lead-shielded and lead-and-polyethylene-shielded cases agree within overlapping error bars.

V. CONCLUSIONS AND ONGOING WORK

The ability of the DPI to detect SNM in the presence of intervening material was tested at the JRC facility in Ispra, Italy. By utilizing both neutron and photon data, the DPI was able to correctly locate the MOX canister in all three shielding configurations tested. When lead shielding was present, neutron imaging was required to locate the source because the photon images were washed out by background radiation. In all cases, the intrinsic resolution of the DPI for SBP caused the hotspot to span a larger area on the image than the expected 3°×7°.

Stochastic reconstruction techniques are being investigated for use with the DPI. It is possible that these techniques will allow for higher-resolution images that are less susceptible to background degradation.

REFERENCES

[1] A. Poitrasson-Rivière, M. C. Hamel, J. K. Polack, M. Flaska, S. D. Clarke, and S. A. Pozzi, “Dual-particle imaging system based on simultaneous detection of photon and neutron collision events,” Nucl. Instr. Meth. A, vol. 760, pp. 40-45, Oct. 2014.

[2] M. C. Hamel, A. Poitrasson-Rivière, J. K. Polack, S. D. Clarke, M. Flaska, and S. A. Pozzi, “Design and analysis of a two-plane dual-particle imaging system,” Proc. of INMM 54th Annual Meeting, Palm Desert, CA, July 2013.

[3] J. K. Polack, A. Poitrasson-Rivière, M. C. Hamel, K. Ide, K. L. McMillan, S. D. Clarke, M. Flaska, and S. A. Pozzi, “Dual-particle imager for standoff detection of special nuclear material,” IEEE Nucl. Sci. Symp. Conf. Rec., Valencia, Spain, Oct. 2012.

[4] M. D. Gerling, J. E. M. Goldsmith, J. S. Brennan, “MINER – A mobile imager of neutrons for emergency responders,” IEEE Nucl. Sci. Symp. Conf. Rec., Seattle, WA, Nov. 2014.

[5] J. M. Ryan, C. Bancroft, P. Bloser, D. Fourguette, L. Larocque, J. Legere, A. Madden, M. L. McConnell, J. Pavlich, G. Ritter, G. Wassick, and M. Rousseau, “An imaging neutron/gamma-ray spectrometer,” Penetrating Radiation Syst. And Applicat. XIII, Proc. of SPIE, vol 8509, 2012.

[6] S. A. Pozzi, E. Padovani and M. Marseguerra, “MCNP-PoliMi: a Monte-Carlo code for correlation measurements,” Nucl. Instrum. Meth. A, vol. 513, pp. 550–558, Nov. 2003.